11-23-1994

Cryo-Jet Preservation of Calcium in the Rat Spinal Cord

William B. Greene
Medical University of South Carolina

Lyle G. Walsh
Medical University of South Carolina

Recommended Citation

Utah State University
MERRILL-CAZIER LIBRARY

CRYO-JET PRESERVATION OF CALCIUM IN THE RAT SPINAL CORD

William B. Greene[*] and Lyle G. Walsh

Medical University of South Carolina, Department of Pathology and Laboratory Medicine,
Charleston, South Carolina 29425

Abstract

In order to determine the distribution of diffusible ions, especially calcium, in rat spinal cord axons before and after trauma, sham, 6 hours post 6 gm/cm and 20 gm/cm trauma cords were cryo-jet frozen *in situ* and cryo-sections were subjected to electron probe X-ray microanalysis. The results confirm part of the Ca hypothesis, i.e., some spinal cord axons accumulate intracellular Ca after traumatic injury. In addition, 6 hours after trauma, Ca is **only** accumulated by axons that have also lost homeostasis. Thus, it is likely that observations of the continual rise of Ca in the traumatized spinal cord are due to an increase in the number of axons that have lost homeostasis rather than an overall increase in Ca within surviving cells.

Key Words: Cryo-jet, cryo-section, freeze substitution, calcium toxicity, spinal cord trauma, myelopathy, X-ray microanalysis.

[*]Address for correspondence:
William B. Greene,
Department of Pathology and Laboratory Medicine
Medical University of South Carolina
171 Ashley Ave
Charleston, SC 29425
 Telephone number: (803) 792-3587
 FAX number: (803) 792-4157

Introduction

The pathologic events of spinal cord trauma can result in varying degrees of necrosis at the site of injury, with permanent neurological impairment. Necrosis, which is the sum of all the degradative changes that take place in cells and tissues after they die, takes time to develop. Except for slight hemorrhages, the cord may reveal no microscopic changes until 6 to 24 hours after trauma. Therefore, there is a considerable latent period between the moment of injury and the onset of necrosis.

This period has been defined in the animal trauma model at 3 to 24 hours. The questions of precisely when the segment of cord dies and whether or not it can be salvaged during the latent period remain unanswered. Research has provided a rational basis for believing that post trauma factors contribute to the permanent functional impairment of the spinal cord. This has given hope that therapies designed to modify the secondary events may lead to significant improvement in the spinal injured patient.

The patterns of necrosis observed in humans can be readily reproduced in the laboratory using animal models of injury which include dropping a known weight from a known height onto a surgically exposed spinal cord (Balentine, 1978; Balentine and Dean, 1982). At the moment of impact and during the primary injury phase, there are changes in the spinal cord which indicate that neural membranes are altered (Banik *et al.*, 1980). In order to develop therapeutic treatment methods, the extent and reversibility of these alterations were investigated by several groups (Green *et al.*, 1985; Noyes, 1987; Saunders *et al.*, 1987; Young, 1985). In the present report, emphasis has been placed on secondary events leading to calcium toxicity. Increased intracellular calcium was previously associated with secondary damage following spinal cord injury (Balentine and Spector, 1977; Schlaepfer, 1979).

Spinal cord, as well as most other tissues suffer immediate and irreparable ischemic damage when removed from the living host for subsequent physical or chemical preservation. Diffusible ions can be shifted well away

from their native positions during the short interval between separation and preservation (Morgan *et al.*, 1978). The most critical step in the preparation of tissue for X-ray microanalysis of diffusible elements is cryo-preservation. The cryo-jet technique is ideal for freezing rat spinal cord segments that cannot be removed from the host animal without severe ionic perturbations. The jet stream hits the entire curvature of the exposed cord surface simultaneously and with maintained force. Tissue samples which were free from discernible freezing artifacts have been documented with propane jet freezing of small droplets of samples between thin layers of conductive material (Burstein and Maurice, 1978; Knoll and Plattner, 1982; Plattner and Knoll, 1984), plunge freezing (Ryan, 1992) or high pressure freezing (Müller and Moor, 1984; Müller *et al.*, 1976). The depth of vitreous freezing is difficult to quantify without performing electron or X-ray diffraction on suitably oriented frozen, hydrated specimens. The problem may be best circumvented by giving measurements for the depth of preservation which is free from discernible freezing damage observable in the microscope following freeze substitution. This depth appears to be normally only 10-20 μm (Angell and Choi, 1986; Costello, 1980; Mayer and Brugeller, 1982; Sitte, 1979) from the surface of biological specimens that are thicker than 40 μm. If a sample is thicker than 40 μm then the center of the specimen cannot be cooled rapidly enough to prevent the growth of ice crystals (Costello and Corless, 1978). For most *in situ* biological samples, vitreous freezing cannot be accomplished. However, freezing is sufficient for compositional analysis when the size of ice crystals is smaller than the smallest structure to be probed.

Although vitrified cells are limited to a predictable and very shallow depth from the tissue surfaces (Haggis, 1986), some deeper tissues, that contain natural cryo-protection such as lipid rich axons, can be useful for microanalysis if the ice crystals remain relatively small (Hereward and Northcote, 1972). In usual practice, we often find acceptably frozen axons for microanalytical purposes, more than 100 μm below the cord surface.

An important factor in any freezing method is the achievable cooling rate. In plunge freezing, it is necessary that the specimen pass rapidly into and continue through a liquid coolant in order to extract heat from the tissue sample caused by the formation of ice crystals (Ryan, 1992; Ryan *et al.*, 1987). This is normally called the latent heat of crystallization and is a major factor affecting the cooling rate. As tissues plunge through a stationary coolant the insulating surface vapor is displaced. Specimens are accelerated through the limits of the plunge (depth versus time) in the attempt to dissipate the latent heat of crystallization. In using the propane jet, the sample is stationary and the column or "tank" of coolant is plunged onto and around the sample achieving the same or a better freezing rate than plunging. The jet blast can last 5 or 10 seconds whereas a plunge is complete in less than a second, depending on the depth of the tank.

In the present study, animals were sacrificed six hours after trauma and axonal profiles in spongioform areas of the cryo-jetted cord were studied by transmission electron microscopy (TEM) and electron probe X-ray microanalysis (EPMA).

Materials and Methods

The cryo-jet

The jet freezing apparatus (Fig. 1) was constructed by the modification of a model 4770 Parr critical point drying bomb (Parr Instrument Co, Moline, IL) and has been described in a previous publication (Greene and Walsh, 1992). An indwelling, resistance thermometer (DP651/661, Omega; Omega, Stamford, CT) with a 20 cm wand type thermistor [Omega Resistance Thermometer Digital (RTD) type] was added so that the tip reached to within 1 cm of the bottom of the reaction vessel). The distal end of the thermistor was secured to the flat surface of the top of the vessel by a pressure fitting. The pressure jet consists of an insulated, low temperature spring valve (Whitey SS-1GS4-LT; Whitey, Solon, OH) with a stainless steel 5 mm orifice tube that is the outlet for pressurized liquid propane. The jet assembly is screwed into the top surface and fastened with a pressure plug. A dip tube extending from the bottom opening of the pressure jet serves to draw up the super cooled liquid propane from the bottom of the chamber. The internal pressure of the chamber is constantly monitored by a low temperature pressure gauge (U.S. Gauge Co., Moline, IL; 316 stainless steel tube socket and tip welded) that is mounted onto the top surface of a stainless steel manifold via a 10 cm long, 7 mm inner diameter tube. The tube connecting the manifold to the chamber top, keeps the main body of the pressure gauge a sufficient distance away to prevent the gauge from freezing. External pressure is supplied from a dry nitrogen cylinder that is fitted with a high pressure regulator (Fisher Scientific, Atlanta, 10-572-1E). A stainless steel flexible hose (Swagelock, Solon, OH) joins the regulator to the manifold valve using the female portion of the quick connect. The hose is connected to a copper coil submerged in liquid nitrogen so that the dry nitrogen used to pressurize the chamber is pre-cooled to prevent sudden increases in temperature. Pressure safety is provided by a blow out device, connected directly to the main body of the manifold valve and in constant series with the reaction vessel. The manifold contains a screw type shut off valve to seal off

Figure 1. Diagrammatic view of the cryo-jet apparatus, the propane jet-freezer.
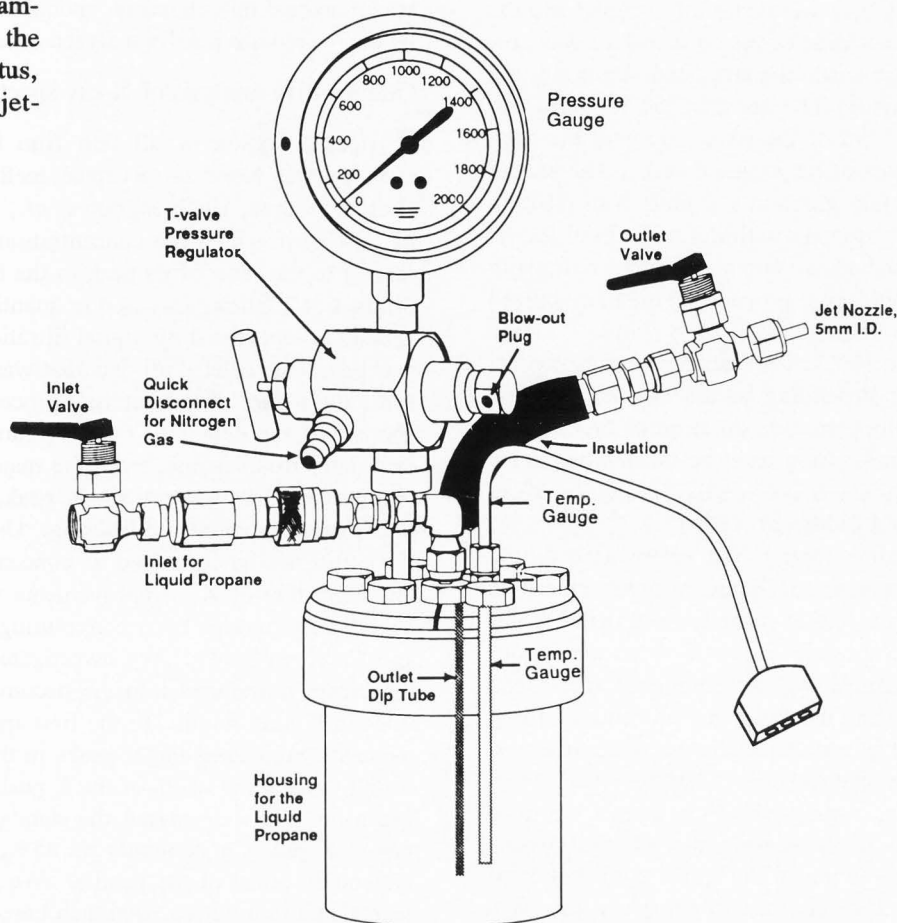
the reaction chamber, however, this valve remains open to the external nitrogen tank during jet operation to repressurize after each blast.

Liquid propane is collected directly into the pre-cooled reaction vessel by passing propane gas under moderate pressure through a coil of 4 mm bore, copper tubing immersed in liquid nitrogen. After collecting 100-125 ml of liquid propane, the vessel is disconnected from the coil and brought to 200 psi (690 kPa) with dry nitrogen through the manifold valve. When the reaction vessel temperature readout reaches -188 to -190°C, jetting can be started.

We estimate, based on our calculations and a chamber pressure of 200 psi (690 kPa), that the propane jet velocity exceeds 100 m/sec at the nozzle tip. The temperature and freezing rate of the tissue sample was also monitored. Microthermocouples of 25 μm constantan, (Costello, 1980) and an Omega model 651 resistance monitor were interfaced to a Zenith PC through an oscilloscope and the following data was collected:

1) Temperature of liquid propane (LP) just at solidification was -191°C; **2)** Temperature of LP at the nozzle (5 mm orifice) at 200 psi (690 kPa) was -195°C; **3)** Temperature of LP 5 mm from the jet nozzle at 200 psi

(690 kPa) was slightly colder; **4)** The cooling rate with the thermocouple placed 5 mm from the nozzle and the pressure set at 200 psi (690 kPa) was 30,000°C per second; **5)** Freezing rate of the sample with the thermocouple placed beneath and in the middle of the sample was approximately the same as in **4**. Our preliminary data shows that pressures higher than 200 psi (690 kPa) do not appreciably alter the freezing rate.

Cryo-jet operation

Sham and experimental rats weighing 250 grams were anesthetized with Ketamine, laminectomies were performed and the dura carefully removed. A 0.5 gram teflon impounder was placed on the exposed dura, and either sham, 6 or 20 gm/cm impact trauma was delivered by sliding an appropriate weight down a rod onto the impounder. The wound was immediately sutured closed. No analgesics were administered. Six hours later the animals were again anesthetized with Ketamine and prepared for jet-freezing. The jet apparatus was cooled, filled with liquid propane and pressurized with dry nitrogen. A short blast of liquid propane from the jet valve cooled the jet nozzle to the proper temperature. The cryogen pressure dropped sharply but recovered immediately. While testing and conditioning the system,

the laminectomy sutures were carefully opened and the cord exposed. Desiccation of the cord surface was prevented by applying a small chamber, containing a saline pad, over the wound. The anesthetized rat was then placed directly in front of the jet nozzle with the blast directed to the center of the exposed cord. The animal was held with a safety glove in a slightly bent position to present the cord squarely within 3 to 5 cm of the jet nozzle. The exposed spinal cord was frozen *in situ* with a jet of super cooled liquid propane. This immobilized all electrolytes in the freezing zone within 1 msec (Greene and Walsh, 1992). Jet-freezing could be repeated 10 to 15 times, depending on the amount of liquid propane used in filling and the duration of the jet blast used for each animal. Care must be taken when using propane in the cryojet to avoid the possibility of an explosion (Ryan and Liddicoat, 1987).

Immediately after jetting, the entire animal was plunged into a container of liquid nitrogen placed in close proximity to the jetting apparatus within the explosion proof hood. Successful removal of the spinal cord from the frozen animal was accomplished more than 2/3rd of the time using the following procedure. First, the glistening, well frozen surface tissues were cut away, **under liquid nitrogen**, using a cutting wheel on a Dremmel tool. The cutting wheel was kept 1 cm from the impact site to avoid heating the adjacent tissue. After the tissue was removed the spinal cord was chipped or sawed out and the ends of the piece of spinal cord were sanded away under liquid nitrogen, until the 3 mm central portion remained. One to two mm blocks for cryo-ultramicrotomy were cleaved from the central portion in the sham animals and from the trauma zone in the experimental animals and stored in cryo-vials under liquid nitrogen.

Electron probe microanalysis (EPMA)

Blocks were frozen onto aluminum stubs using anhydrous heptane and 200 nm thick sections were cut *en face* at -120°C in a Reichert Ultracut IV. The sections were placed on carbon coated, folding copper grids and stored under liquid nitrogen. Grids were transferred to a Be-tipped, Gatan analytical cold stage, placed in an Hitachi H-7000 electron microscope, freeze dried at -100°C to -80°C and analyzed at -100°C. Specimens were analyzed at 125 kV in the scanning TEM (STEM) mode with a 2-4 nA beam (beam current was calculated from screen current measurements that were previously calibrated using a Faraday cup stage). Spectra were collected for 400 seconds live time, using a horizontal KEVEX 30 mm² SiLi detector which has 159.6 eV resolution, measured at the Mn Kα, 1000 cps, using Mn evaporated onto a formvar film on a Be grid. Spectra were analyzed using a KEVEX Delta IV analyzer. Axo-

plasm, axonal mitochondria, endoplasmic reticulum and myelin were individually analyzed in each trauma group.

Quantitative analysis of X-ray spectra

Quantification of all thin film biological EPMA analyses was based on accepted methods (Hall, 1979; Hall and Gupta, 1982; Ingram *et al.*, 1988; Shuman, *et al.*, 1976) in which the concentration of an element is related to the ratio of its peak to the background X-ray production. During one step in quantification the background is suppressed by digital filtration. The old analysis programs deleted all data that was negative. However, the nature of the filtering process is to transform about half the data into negative numbers. This was especially troublesome, since the major Ca X-ray peak overlaps with a region of the K peak, this always produces negative counts on filtering. Using this program, Ca could not be measured at concentrations less than one-tenth that of K. Improvements were made in the analytical programs by deconvoluting the overlap of K and Ca X-ray peaks. We investigated ways to correct the errors introduced into the deconvolution by variations in K peak width. In the first approach we mathematically broadened the K peaks in the reference spectrum to match the width of the K peaks in the specimen spectrum. This decreased the standard error of Ca in mixed K plus Ca standards by 25%, but introduced a systematic offset in the results. We then introduced a second, more intuitive, approach based on the influence of peak width on peak shape. Residuals left after fitting 56 spectra of K standards that had variable K peak widths were summed. The shape of the residual was uniform and reproducible with broader K peaks producing a larger residual. When we included the summed residual spectrum in K-Ca peak deconvolution as if it were an element, the standard error for Ca measurement was significantly reduced without any offset (Walsh and Greene, 1991).

Spectral deconvolution using residuals has not been previously reported. Developing this deconvolution method was an important advance for our EPMA measurements, since it is faster, simpler and more accurate than previous methods which account for shifts in peak width (Walsh and Greene, 1991).

Our spectrum fitting procedure involves several steps. First, a film spectrum, acquired near the current analysis site, is subtracted. Second, the specimen spectrum is recalibrated so that its Kα centroid is within 0.1 eV of the K "shape" standard. Peak centroid position is located by subtracting the background from a copy of the spectrum, under the K and Cu peaks, and then modelling these peaks with computer generated Gaussian peaks. The escape peaks are then subtracted from the original spectrum and the gain and zero of the spectrum
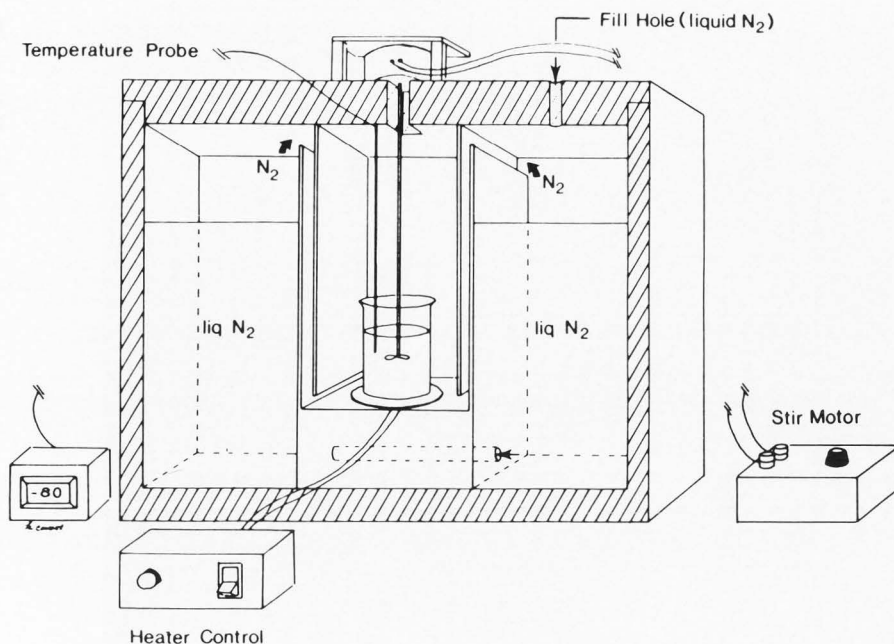
Figure 2. Diagrammatic view of the freeze substitution apparatus.

----

is shifted appropriately. We have previously shown that this recalibration markedly improves deconvolution of the K and Ca overlap (Walsh and Greene, 1991).

Third, the contribution to the spectrum that arises from the grid bars is removed by subtracting a "grid" spectrum that is normalized to the Cu Kα peak. The "grid" spectrum was produced by acquiring a spectrum from a carbon particle that was located close to a grid bar and subtracting a spectrum from an identical particle acquired in the middle of the grid square. The remainder of the spectrum is the component that is due to scattering of electrons into the grid bar. This includes Cu K and L peaks and a significant background.

Fourth, the continuum region integral is measured. We use the region from 4.6 to 6.1 keV because it is devoid of peaks and the contribution from the grid bars is readily removed.

Fifth, multiple least square fits are made with the filtered "shape" standard spectra. We typically include a filtered K residual spectrum to improve deconvolution of K and Ca if the spectrum has a high K content.

Sixth, concentrations are then calculated from the k-ratios (an element's peak integral in the unknown sample, relative to the standard peak counts, which is a good first approximation of the elemental concentration) and proportionality constants and corrected for their mean (Z^2/A, Z = the atomic number, A = absorption within the sample and detector).

Standards

Large quantitation errors, up to 65%, were introduced by following established methods for analysis of standards. Traditional standards of salt solutions in an organic matrix exhibited variable sensitivity to mass loss during analyses that depended on the salt composition of the standard. This had not been previously reported. None of the standards were a good match for tissue.

We established a procedure for minimizing this variability by using three different types of standards, i.e., "shape", "absolute" and "relative" standards. The "shape" standards were thin slivers of mixed salts. The "relative" standards were freeze dried cryo-sections of dextran containing known stoichiometries of mixed salts, always including K. The "absolute" standard was the K content of human red blood cells (RBC). The RBC standard composition was more similar to tissue than any artificial standards. "Relative" standards were used in conjunction with an "absolute" standard to reduce the errors in EPMA due to differences among mass loss from the standards and from the specimens. "Shape" standards were used for fitting spectra to facilitate deconvolution of overlapping peaks.

In addition, a modification of the "Hall" approach to EPMA quantification was made in which the k-ratio was used. This eliminated the need for repeated measurement of the standards' continuum integrals during quantification.

Freeze substitution

In order to monitor the success of cryo-jet freezing, samples were routinely freeze substituted and processed for electron microscopy. A previously described freeze substitution methodology (Greene and Walsh, 1992) of our own design (Fig. 2), where the temperature of the
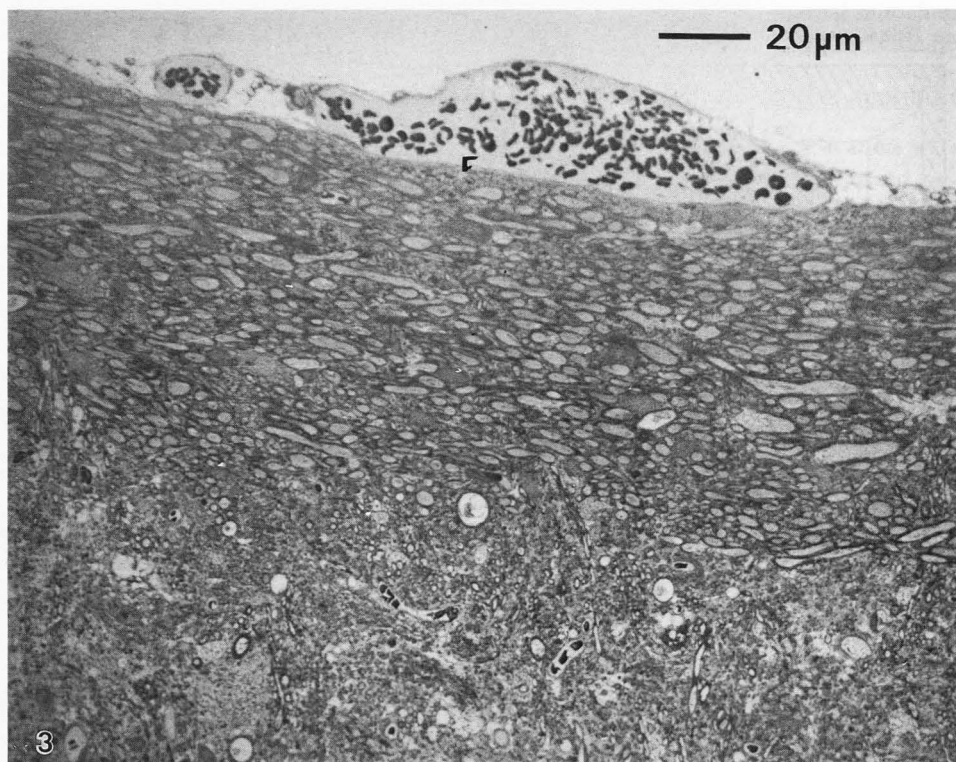
Figure 3. Freeze substitution of cryojetted rat spinal cord. Epoxy resin section. Toluidine blue stained.

substituting fluid is controlled, was used.

The prototype freeze substitution apparatus was made from a styrofoam shipping container [7.5 x 10.5 x 10.5 inches (19 x 26.5 x 26.5 cm)] with 2 inch (5.1 cm) walls. The inner substitution chamber is 7.5 x 2.5 x 5.5 inches (19 x 6.3 x 14 cm) deep. Flow of cold nitrogen gas is controlled by the placement of stationary panels, which form the wall of the liquid nitrogen well, and adjustable panels, after the method of Sitte (1982). The stationary panels are glued vertically with a 0.5 inch (1.25 cm) gap from the top of the stationary panel to the top of the box. The cold gas evolved from the liquid nitrogen flows over the top of the stationary panel and then to the bottom of the reaction vessel through a space formed by the adjustable panels. The gap at the bottom of each adjustable panel can be altered to control the flow of gas into the reaction chamber which governs, to some extent, the convective cooling of the reaction chamber.

An externally controlled heating plate is located just under the cold acetone containing vessel at the floor of the reaction chamber to heat the substituting fluid and nitrogen gas to the desired temperature. The temperature of this plate is adjusted to keep the substituting fluid at the desired temperature (a constant -85°C for most of the substitution run). Adjustments of the plate temperature are usually not necessary after the first half hour of operation except when warming the vessel or after filling the liquid nitrogen chambers. The temperature of the

acetone is monitored by the placement of an RTD wand directly into the plastic substitution vessel.

In order to maintain laminar flow of the nitrogen gas, the system is closed off tightly at the top by the cover of the styrofoam container. A port in the cover permits access and placement of the temperature probe and the stirrer. Holes are cut into the styrofoam cover directly over the liquid nitrogen containers for refilling with liquid nitrogen. These holes are kept plugged with #2 rubber stoppers when not in use. The depth of the liquid nitrogen can be periodically checked by inserting a wet dip stick to the bottom of the container and noting how high the water freezes.

The second most important component of good freeze substitution, after temperature control, is constant agitation of the substitution medium. Water (ice) is extracted from the frozen tissues much more efficiently if the interfacing coolant is in motion. This is easily accomplished by placing a motor driven propeller into the top one-third of the substituting fluid and stirring slowly throughout the procedure. Pre-cooled, substitution media must be replaced at regular intervals, since it gains water from the tissue and loses substitution efficiency (Humbel and Müller, 1986).

Protocol

1. Bring the reaction chamber of the freeze substitution box to a stable balanced -85°C using the methods described above.

Figure 4. Representative conventional TEM image of freeze substitution. Sham operated.
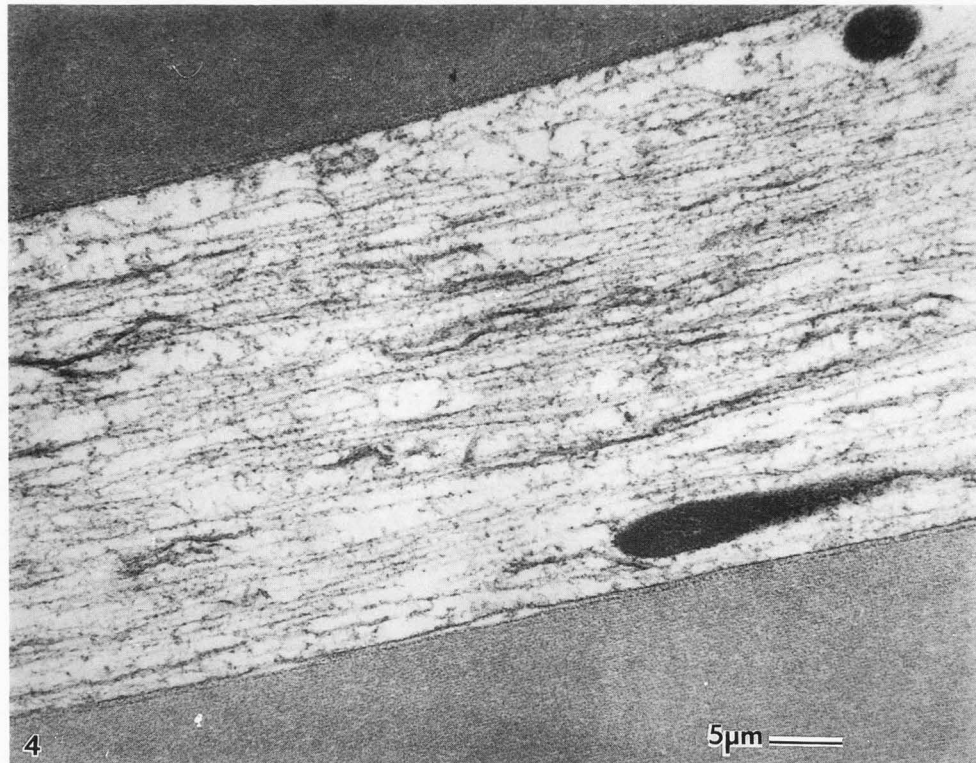
2. Add 80 ml of fresh, spectroscopic grade acetone to a plastic container (Fisher specimen container 128 ml cat. #14-375-110A).

3. Add 3-4 grams of baked molecular sieve (Fluka cat. # 69839) to the cold acetone. Cap and shake gently to expose all the acetone to the molecular sieves.

4. Place the acetone container into liquid nitrogen and bring the temperature to -85°C. Monitor the temperature with the RTD rod through a snug opening in the cap.

5. When the acetone has reached the proper temperature, place the container into the freeze substitution chamber.

6. Place the temperature probe wand into the cold acetone through the access opening in the styrofoam top. Make sure the rod is placed to one side of the container so as to avoid contact with the stirring propeller.

7. Place the stirring propeller into the center of the acetone container, 2/3rd from the bottom of the liquid.

8. Begin stirring. The solution should quickly equilibrate to the proper substitution temperature.

9. Transfer frozen tissue from liquid nitrogen storage into -85°C acetone in reaction chamber.

10. Continue stirring and replace the substitution fluid every 6-8 hours.

11. Monitor the temperature and adjust as needed. Osmium tetroxide crystals or uranyl acetate may be dissolved in the cold acetone for fixation and block staining if desired.

12. When substitution is complete (24-48 hours) the specimens can be gradually warmed to room temperature by adjusting the temperature of the nitrogen gas heating plate (and lowering the level of liquid nitrogen) **or**

a. Remove the thermometer and stir rod.

b. Replace the cap on the acetone container and remove it from the reaction chamber.

c. Place the closed container into a styrofoam cooler containing 4 pounds of dry ice and allow the ice to sublimate to ambient temperature (24-36 hours).

13. After reaching room temperature, change the acetone twice.

14. Process the tissues using propylene oxide, infiltrate with resin and embed as usual.

Spinal cords that were cryo-fixed in the above described manner and processed for freeze substitution exhibited excellent preservation. Thick, toluidine blue sections showed that the depth of acceptable freezing appeared to be in excess of 50 μm (Fig. 3). Thin sections of sham operated and traumatized axons showed good morphological detail as well (Fig. 4).

Results

Twenty axonal profiles from each of 2 blocks, taken from 10 animals in each group were examined (400 spectra each in the sham operated, 6 gm/cm and 20 gm/cm groups). Elemental composition was measured by EPMA in the axoplasm, mitochondria, endoplasmic

Table 1. Elemental composition of dorsal axons 6 hours after sham trauma. Values are means ± standard error of mean (sem); units are mmoles/kg dry weight. Cont. = Continuum.

	Axoplasm	ER	Mitochondria	Myelin
Na	96 ± 13	153 ± 26	85 ± 13	68 ± 4
P	259 ± 25	390 ± 50	353 ± 17	450 ± 12
Cl	219 ± 27	349 ± 66	198 ± 19	32 ± 3
K	1027 ± 106	1704 ± 304	886 ± 69	105 ± 10
Mg	20.0 ± 2.6	27.0 ± 5.1	27.6 ± 2.4	15.1 ± 1.0
Ca	6.3 ± 1.0	12.5 ± 2.8	4.1 ± 0.8	3.0 ± 0.3
Fe	6.7 ± 1.4	6.1 ± 2.1	8.5 ± 0.9	6.4 ± 0.5
Cont.	25 ± 3	33 ± 11	59 ± 6	134 ± 13

Table 2. Elemental composition of swollen axons 6 hours after 6 gm/cm trauma. Values are means ± sem; units are mmoles/kg dry weight. Cont. = Continuum.

|	Axoplasm	ER	Mitochondria	Myelin
Na	130 ± 22	162 ± 23	168 ± 37	71 ± 4
P	451 ± 57	461 ± 57	454 ± 33	488 ± 11
Cl	467 ± 59	354 ± 46	314 ± 43	58 ± 5
K	1760 ± 134	1438 ± 181	1159 ± 127	133 ± 6
Mg	47.1 ± 7.6	42.3 ± 3.9	29.7 ± 3.1	15.0 ± 2.4
Ca	6.7 ± 2.4	6.6 ± 1.4	4.4 ± 1.1	3.4 ± 0.3
Fe	0.6 ± 2.4	1.6 ± 1.8	0.5 ± 2.2	4.5 ± 0.4
Cont.	10 ± 1	19 ± 2	22 ± 3	133 ± 6

Table 3. Elemental composition of swollen axons 20 hours after 20 gm/cm sham trauma. Values are means ± sem; units are mmoles/kg dry weight. Cont. = Continuum.

	Axoplasm	ER	Mitochondria	Myelin
Na	55 ± 18	59 ± 4	55 ± 8	43 ± 3
P	367 ± 30	328 ± 27	343 ± 35	371 ± 17
Cl	421 ± 28	181 ± 26	120 ± 11	47 ± 6
K	1620 ± 121	878 ± 124	667 ± 80	135 ± 10
Mg	37.1 ± 5.6	22.8 ± 2.8	19.8 ± 2.7	12.8 ± 0.9
Ca	5.2 ± 2.5	2.3 ± 1.0	2.6 ± 0.7	2.3 ± 0.3
Fe	17.7 ± 7.9	8.4 ± 2.5	5.1 ± 2.0	6.4 ± 1.7
Cont.	16 ± 2	26 ± 2	34 ± 6	75 ± 7

reticulum (ER), and myelin sheath in superficial axons of the dorsal columns in sham operated, 6 gm/cm and 20 gm/cm impact trauma spinal cords. In probing the axoplasm, the probe area window was set to cover as large an area as possible. If a large phosphorus peak appeared, the window size was reduced to avoid the myelin sheath. Spectra that showed large copper peaks were discontinued and other suitable axons were found (away from the grid bar or out of the shadow). Strict criteria for normally appearing, non-swollen shams were adhered to (Fig. 5).

Sham axons

The elemental composition of axoplasm, axonal mitochondria, axonal ER and myelin from shams (Table 1) is similar to that measured by EPMA of cardiac muscle (Walsh and Tormey, 1988a,b) and epithelia (Mason et al., 1981). The major differences in concentration among compartments is due to the amount of hydration. For instance, mitochondria are more dense than axoplasm and have a lower water content. Consequently, when two structures with identical K ionic activities are analyzed, the less dense structure will have a higher K concentration, as measured by EPMA. This makes EPMA especially useful for identifying changes in hydration, due to swelling, and for measuring sequestration, where the element is bound and the cell content rises while the ionic activity in the cytoplasm is not changed.

Measurements of sham K/Na and K/P (10.7 and 4.0 mmoles/kg) agrees well with other studies of EPMA of spinal cord, sciatic and optic nerve (9.7 and 4.6 mmoles/kg) (LoPachin et al., 1988, 1989, 1990, 1991). The Ca content of sham animals was low in all areas measured except the ER, which is about twice that of the surrounding axoplasm. Ca sequestration by ER has been found in muscle (Wheeler-Clark and Tormey, 1985) and photoreceptors (Baumann et al., 1991) and is important for normal protein packaging and axonal transport (Lasek and Hoffman, 1976).

Myelin was the most dense structure analyzed, as indicated by the high continuum values. The concentrations of Na, Mg, P and Ca are all only slightly lower in myelin than those of the axoplasm and axonal mitochondria. However, myelin Cl is only one-seventh and myelin K is only one-tenth the concentration measured in axoplasm. This difference is not due to K and Cl depletion from the cytoplasm within the myelin. Instead, it reflects the fact that the majority of the Na, Mg, P, and Ca within any cell is bound to dry mass, i.e., proteins, carbohydrates and lipids (Rick et al., 1982). The amount of this binding is similar in most compartments and consequently, so are the concentrations of these elements as measured by EPMA. In contrast, only about

Figure 5. Typical cryo-jetted rat spinal cord. Sham, longitudinal section. Freeze dried, fresh frozen, not freeze substituted. Polaroid photograph taken directly from the cathode ray tube.
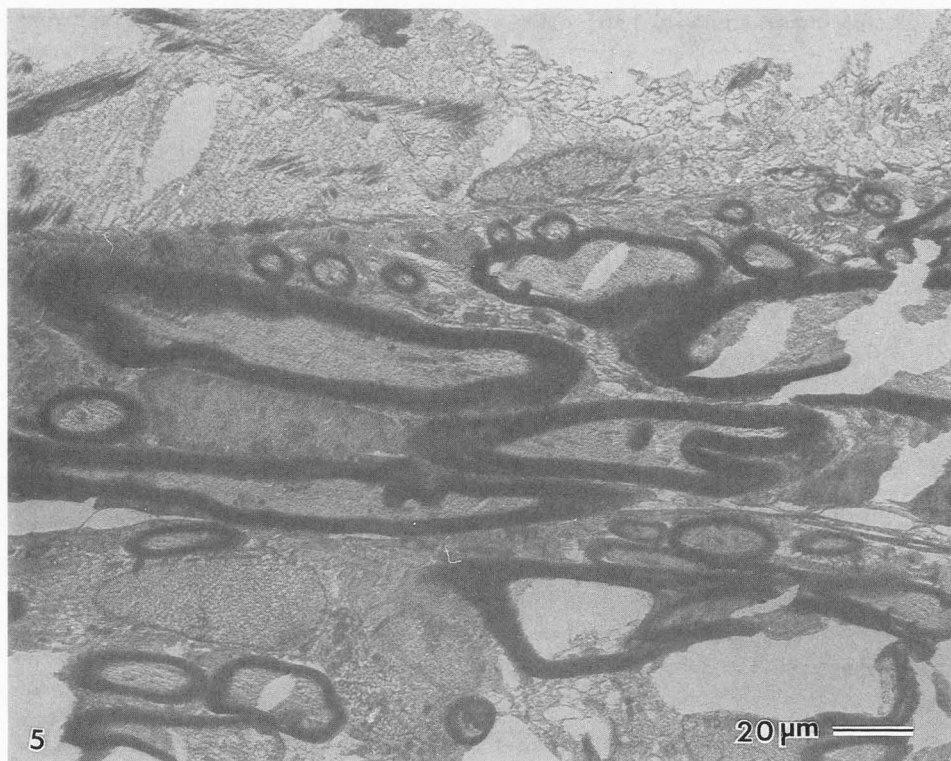
one-third of the K and Cl is bound; the rest being ionic. Structures that are more dense, such as myelin, have a smaller aqueous fraction and the elements most associated with the aqueous fraction, i.e., K and Cl, make up a smaller proportion of the total content.

Heterogeneous axons

This study is the first to directly measure the subcellular electrolyte shifts in CNS trauma. Previous EPMA studies of axotomy and ischemia reported a uniform axonal response (LoPachin *et al.*, 1989). However the morphology of trauma and previous EPMA studies of cardiac reperfusion injury (Walsh and Tormey, 1988a,b) indicated that pathological damage in excitable tissues is often very heterogeneous. The present study was designed to characterize the cellular responses of the spinal cord white matter, specifically looking for a heterogeneous response to trauma. EPMA of low levels of Ca requires long analyses of each single organelle which limits the number of axons that can be analyzed. Therefore, no effort was made to randomly sample axons. Instead, equal numbers of nearly normal axons were compared with axons exhibiting deranged morphology or altered chemical composition.

The axonal changes from impact trauma were markedly heterogeneous at both the morphological and chemical compositional level. Adjacent axons can have very different composition. Fortunately, while there is a continuum of morphological damage, the elemental shifts are stereotypic. After the analyses were completed, axons were grouped according to their K and Na content. The first has low Na and high K; the second has low Na and low K; the third group has high Na and low K. All subsequent analyses were made on each population of axons according to these 3 groupings.

Swollen axons

Since the trauma force was mild to moderate, it is not surprising that most axons had only minor elemental shifts 6 hours after trauma. Based on axoplasm with high K and low Na, the swollen axon group was the same for 6 and for 20 gm/cm trauma (Tables 2 and 3). The axoplasm has natural variability, consequently, the K content relative to dry mass is variable. The variability of K in swollen axons was larger but not significantly different than in shams.

Axonal swelling resulted in decreased density and increased K. The Na/K pumps maintained the ionic equilibrium and K accompanied the flow of water into the axoplasm. As with myelin, the axoplasmic Cl content rose in parallel with K while the concentrations of the predominantly bound elements, i.e., Na, Mg, P and Ca had a slight change. The mitochondria in this group showed some signs of swelling. Myelin was significantly swollen with increased K and Cl and decreased density.

The other significant compositional shift found in swollen axons was decreased Ca in the ER, indicating a

595

Table 4. Elemental composition of condensed axoplasm 6 hours after 6 and 20 gm/cm trauma. Values are means ± sem, units are mmoles/kg dry weight.

	20 gm/cm	6 gm/cm
Na	61 ± 15	109 ± 13
P	289 ± 33	262 ± 29
Cl	109 ± 10	136 ± 15
K	403 ± 34	289 ± 31
Mg	13.4 ± 2.1	17.8 ± 2.7
Ca	1.8 ± 0.7	4.7 ± 0.9
Fe	6.0 ± 6.0	4.1 ± 4.1
Continuum	23 ± 1	34 ± 13

Table 5. Elemental composition of non-functional axons 6 hours after 20 gm/cm trauma. Values are means ± sem; units are mmoles/kg dry weight. Cont. = Continuum.

	Axoplasm	ER	Mitochondria	Myelin
Na	1694 ± 588	1278 ± 418	1752 ± 492	265 ± 29
P	500 ± 176	260 ± 51	386 ± 112	418 ± 17
Cl	916 ± 429	611 ± 221	868 ± 397	91 ± 28
K	102 ± 28	220 ± 90	117 ± 24	36 ± 6
Mg	26.3 ± 3.0	17.7 ± 7.6	24.5 ± 18.2	4.7 ± 2.1
Ca	66.5 ± 12	51.7 ± 19.5	74.9 ± 17.1	15.8 ± 1.7
Fe	22.4 ± 6.0	23.1 ± 3.8	24.3 ± 7.3	10.8 ± 1.3
Cont.	10 ± 2	16 ± 3	25 ± 11	74 ± 11

sustained impairment in ER function while other homeostatic mechanisms remained nearly normal. However, the volume of axoplasmic ER is so low that even if all of the sequestered Ca were released at once, it would have only a transitory impact on total axoplasmic Ca.

Condensed axons

The second population of axons in both 6 and 20 gm/cm trauma were condensed (Table 4) with an increased axoplasmic continuum count rate. The axoplasmic concentrations of the predominantly bound elements, Na, Mg, P, and Ca, were slightly different from shams or swollen axons. However, both K and Cl were significantly lower than in shams or swollen axons.

The mitochondria and ER of condensed axons were no different than in swollen axons and their values are reported together. Similarly, the myelin of both swollen and condensed axons was swollen and the data were grouped together (Table 2).

Non-functional

The third population, chemically non-functional axons, was only found in spinal cords subjected to 20 gm/cm trauma and had lost homeostasis (Table 5). All compartments of the non-functional axons and their associated myelin lost most of their K and accumulated large amounts of Na, Cl and Ca. The 10 fold increase in axoplasmic Na and Ca matches interstitial values found in peripheral nerve (LoPachin et al., 1989) indicating that these axons are at equilibrium with the interstitium. However, in contrast to peripheral nerve the interstitial volume of the dorsal tracts, even after moderate trauma, was too small and indistinct to be readily analyzed. All non-functional axons had myelin with low K, and high Na and Ca. Myelin with these electrolyte shifts was never found around swollen or condensed axons. The myelin, however, never accumulated as much Ca as the axonal compartments.

In spite of the well known ability of mitochondria to take up Ca, there is no evidence for greater Ca accumulation within mitochondria or ER in the axoplasm of chemically non-functional axons.

Morphology

In order to perform EPMA analyses, the beam current and configuration of the electron microscope are not optimized for viewing. Our samples are unstained, consequently, small structures such as individual neurofilaments or myelin lamellae were not resolved during analyses.

A surprising finding of this study was the inability to predict by inspection which axons were only swollen and which were chemically non-functional. Many axons, that looked nearly normal, exhibited the elemental shifts indicative of swelling. All axons that were dense, exhibited condensation and many of the axons with morphological damage were chemically non-functional. However, about half of the swollen axons had intact electrolyte gradients. Conversely, many of the chemically non-functional axons showed few signs of morphological damage. Therefore, 6 hours after trauma, axonal morphology cannot be used to predict axonal vitality or electrolyte composition.

All values expressed in tables are the mean ± the standard error of the mean. Tests for significant difference at P ≤ 0.05 are students t-tests using modified values of t for multiple comparisons based on Sidak's multiplicative inequality (Sokal and Rohlf, 1981).

Discussion

Calcium toxicity has been the major interest in our laboratory because of the occurrence of selective axonal calcification and nerve fiber changes (granular axoplasm, vesicular myelin) attributable to calcium activated neutral

proteases. We have also noted a progressive increase in total tissue calcium in our experimental model of rat spinal cord trauma. Calcium induced myelopathy, when viewed as the primary injury, is morphologically comparable to the primary injury of trauma. The primary injuries initiated by trauma cause a wide range of electrolyte shifts among the subcellular organelles of axons. These shifts are different and more variable than secondary shifts and they directly induce predictable secondary injuries. Secondary injuries cause a progression of intra- and intercellular electrolyte shifts that determine the recovery or death of individual axons after trauma.

Electrolyte shifts indicative of secondary injuries can be ameliorated with specific treatments. For example: antioxidants, such as methylprednisolone and amino steroids, prevent general dissipation of ionic gradients and high doses of Ca channel blockers, e.g., Flunarazine, inhibit the release of ER Ca during trauma and help maintain ER Ca sequestration after trauma (Black *et al.*, 1991; Bracken *et al.*, 1990).

An unexpected finding, that major morphological changes, such as adaxonal swelling and vesicular demyelination, which are the hallmarks of spinal cord trauma, were not indicative of electrolyte imbalance. Conversely, large shifts in diffusible ion concentrations was not always accompanied by extensive morphological damage. Several papers have discussed calcium toxicity as a secondary injury in human cases and animal models and have described the typical altered morphology that occurs during the first several hours post trauma (Balentine, 1985; Balentine and Greene, 1984). Based on these previous morphological findings and a comparison to the shifts in diffusible ions reported here, we feel that clinical trials using calcium antagonists will have increased success (Balentine, 1985; Black *et al.*, 1991; Bracken *et al.*, 1990; Young and Flamm, 1982). While the chemical and morphological composition is likely to change with time after trauma, the 6 hour post trauma studies are encouraging because changes that were previously considered to be irreversible (Balentine, 1985) may prove to be repairable.

In conclusion, we have found three types of axons after trauma: 1) swollen, with increased axoplasmic K and decreased density, 2) condensed, with the exclusion of K rich cytosol by condensed axoplasm and 3) chemically non-functional, with loss of all electrolyte gradients. Ca was only accumulated by the non-functional axons. Unlike shams, the ER of swollen or condensed axons had no sequestered Ca. The response of axons and the associated myelin was paired, i.e., loss of homeostasis within the axon was always accompanied by loss of homeostasis in the myelin and vice versa. Morphology did not predict chemical derangement. Axons with morphology ranging from nearly normal to badly damaged could be found with loss of homeostasis.

The similarity between 6 and 20 gm/cm trauma lends hope to further studies and treatments. Swelling and condensation have been found to be common responses to both. Consequently, studies of recovery from mild injury have meaning for more severe trauma. Since the spinal cord recovers spontaneously from mild trauma, and since the functional axons after 6 hours have a similar composition in both levels of injury, then there is every reason to believe that the recovery of the remaining functional axons can be as complete in severe as in mild trauma.

Acknowledgments

References

Angell CA, Choi Y. (1986) Crystallization and vitrification in aqueous systems. J. Microsc. **141**: 251-261.

Balentine JD. (1978) Pathology of experimental spinal cord trauma. II. Ultrastructure of axons and myelin. Lab. Invest. **39**: 254-266.

Balentine JD. (1985) Hypotheses in spinal cord trauma research. In: Central Nervous System Trauma Status Report. Becker DP, Povlishock JT (eds.). North-Holland Publishing Co, NY. 455-461.

Balentine JD, Dean DL. (1982) Calcium induced spongioform and necrotizing myelopathy. Lab. Invest. **47**: 286-295.

Balentine JD, Greene WB. (1984) Ultrastructural pathology of nerve fibers in calcium-induced myelopathy. J. Neuropath. Exp. Neurol. **43**: 500-510.

Balentine JD, Spector M. (1977) Calcification of axons in experimental spinal cord trauma. Ann. Neurol. **2**: 520-552.

Banik NL, Powers JM, Hogan EL. (1980) Effects of spinal cord trauma on myelin. J. Neuropathol. Exp. Neurol. **139**: 232-244.

Baumann O, Walz B, Somlyo AV, Somlyo AP. (1991) Electron probe microanalysis of calcium release and magnesium uptake by endoplasmic reticulum in bee photoreceptors. Proc. Natl. Acad. Sci. **88**: 741-744.

Black P, Markowitz RS, Gillespie JA, Finkelstein SD. (1991) Naloxone and experimental spinal cord injury: effect of varying dose and intensity of injury. J. Neurotrauma **8**: 157-171.

Bracken MB, Shepard MJ, Collins WF. (1990) A randomized, controlled trial of methylprednisolone or naloxone in the treatment of acute spinal cord injury.

New Eng. J. Med. **322**: 1405-1411.

Burstein NL, Maurice DM. (1978) Cryofixation of tissue surfaces by a propane jet for electron microscopy. Micron **9**: 191-198.

Costello MJ. (1980) Ultra-rapid freezing of thin biological samples. Scanning Electron Microsc. **1980**;II: 361-370.

Costello MJ, Corless JM. (1978) The direct measurement of temperature changes within freeze-fracture specimens during rapid quenching in liquid coolants. J. Microsc. **112**: 17-37.

Greene WB, Walsh LG. (1992) An improved cryo-jet freezing method. J. Microsc. **166**: 207-218.

Green BA, Klose KJ, Goldberg ML. (1985) Clinical and research considerations in spinal cord injury. In: Central Nervous System Trauma Status Report. Becker DP, Povlishock JT (eds.). North-Holland Publishing Company, NY. 341-368.

Haggis GH. (1986) Study of the conditions necessary for propane-jet freezing of fresh biological tissues without detectable ice formation. J. Microsc. **143**: 275-282.

Hall TA. (1979) Biological X-ray microanalysis. J. Microsc. **117**: 145-163.

Hall TA, Gupta BL. (1982) Quantification for the X-ray microanalysis of cryosections. J. Microsc. **126**: 333-345.

Hereward FV, Northcote DH. (1972) A simple freeze substitution method for the study of ultrastructure of plant tissues. Exp. Cell. Res. **70**: 73-80.

Humbel BM, Müller M. (1986) Freeze-substitution and low temperature embedding. In: The Science of Biological Specimen Preparation. Müller M, Becker RP, Boyde A, Wolosewick JJ (eds.). SEM, Inc., A.M.F. O'Hare, IL. 175-183.

Ingram P, LeFurgey A, Davilla SD. (1988) Quantitative elemental X-ray imaging of biological cryosections. In: Microbeam Analysis. San Francisco Press. 433-439.

Knoll G, Plattner H. (1982) A simple sandwich cryogen-jet procedure with high cooling rates for cryofixation of biological materials in the native state. Protoplasm **111**: 161-176.

Lasek RJ, Hoffman PN. (1976) The neuronal cytoskeleton, axonal transport and axonal growth. In: Cell Motility, book C: Microtubules and related proteins. Goldman R, Pollard T, Rosenbaum J (eds.). Cold Spring Harbor Laboratory, NY. 1021-1049.

LoPachin RM, Lowery J, Eichberg J, Kirkpatrick JB, Cartwright J, Saubermann AJ. (1988) Distribution of elements in rat peripheral axons and nerve cell bodies determined by x-ray microprobe analysis. J. Neurochem. **51**: 764-775.

LoPachin RM, Lopachin VR, Saubermann AJ. (1989) X-ray microprobe analysis of subcellular elemental distribution in normal and injured peripheral nerve axons. In: Cell Calcium Metabolism. Fiskum G (ed.). Plenum Publishing Corp., New York. 479-489.

LoPachin RM, LoPachin VR, Saubermann AJ. (1990) Effects of axotomy on distribution and concentration of elements in rat sciatic nerve. J. Neurochem. **54**: 320-332.

LoPachin RM, Castaglia CM, Saubermann AJ. (1991) Elemental composition and water content of myelinated axons and glial cells in rat central nervous system. Brain Res. **549**: 253-259.

Mason J, Beck F, Dörge A, Rick R, Thurau K. (1981) Intracellular electrolyte composition following renal ischemia. Kidney Intl. **20**: 61-70.

Mayer E, Brugeller P. (1982) Vitrification of pure liquid water by high pressure jet freezing. Nature **298**: 715-718.

Morgan AJ, Davies TW, Erasmus DA. (1978) Specimen preparation. In: Electron Probe Microanalysis in Biology. Erasmus DA (ed.). Chapman and Hall, London. 94-99.

Müller M, Moor H. (1984) Cryofixation of thick specimens by high pressure freezing. In: Science of Biological Specimen Preparation for Microscopy and Microanalysis. Revel JP, Barnard T, Haggis GH (eds.). Scanning Electron Microscopy, Inc. AMF O'Hare, IL. 131-138.

Müller M, Meister N, Moor H. (1976) Freezing in a propane jet and it's application in freeze-fracturing. Mikroskopie (Wien), **36**: 129-132.

Noyes DH. (1987) Correlation between parameters of spinal cord impact and resultant injury. Exp. Neurol. **95**: 535-547.

Plattner H, Knoll G. (1984) Cryofixation of biological materials for electron microscopy by the methods of spray-sandwich, cryogen-jet and sandwich-cryo-jet freezing: A comparison of techniques. In: Science of Biological Specimen Preparation for Microscopy and Microanalysis. Revel JP, Barnard T, Haggis GH (eds.). Scanning Electron Microscopy, Inc. AMF O'Hare, IL. 139-146.

Rick R, Dörge A, Thurau K. (Microsc.1982) Quantitative analysis of electrolytes in frozen dried sections. J. **125**: 239-247.

Ryan KP. (1992) Cryofixation of tissues for electron microscopy: A review of plunge cooling methods. Scanning Microsc. **6**: 715-43.

Ryan KP, Liddicoat MI. (1987) Safety considerations regarding the use of propane and other liquefied gases as coolants for rapid freezing purposes. J. Microsc. **147**: 337-340.

Ryan KP, Purse DH, Robinson SG, Wood JW. (1987) The relative efficiency of cryogens used for

plunge-cooling biological specimens. J. Microsc. **145**: 89-96.

Saunders RD, Brandon YW, DeVries GH. (1987) Effects of methylprednisolone and the combination of alpha-tocopherol and selenium on arachidonic acid metabolism and lipid peroxidation in traumatized spinal cord tissue. J. Neurochem. **49**: 24-31.

Schlaepfer WW. (1979) Nature of mammalian neurofilaments and their breakdown by calcium. In: Progress in Neuropathology. Zimmerman HM (ed.). Raven Press, New York. 101-123.

Shuman H, Somlyo AV, Somlyo AP. (1976) Quantitative electron probe microanalysis of biological thin sections: methods and validity. Ultramicrosc. **1**: 317-339.

Sitte H. (1979) Cryofixation in biological material without pretreatment. A review. Mikroskopie (Wien), **35**: 14-20.

Sokal RR, Rohlf FJ. (1981) Biometry. W.H. Freeman, San Francisco. 208-271.

Walsh LG, Greene WB. (1991) Improved deconvolution of K and Ca by fitting with the K residual. Microbeam Analysis. San Francisco Press. **21**: 13-16.

Walsh LG, Tormey JM. (1988a) Subcellular electrolyte shifts during in vitro myocardial ischemia and reperfusion. Am. J. Physiol. **255**: H917-H928.

Walsh LG, Tormey JM. (1988b) Cellular compartmentation in ischemic myocardium: indirect analysis by electron probe. Am. J. Physiol. **255**: H929-H936.

Wheeler-Clark ES, Tormey JM. (1985) Redistribution of subcellular electrolytes accompanying the increased myocardial contractility produced by low Na. Microbeam Analysis. San Francisco Press. 116-118.

Young W. (1985) Blood flow, metabolic and neurophysiological mechanisms in spinal cord injury. In: Central Nervous System Trauma Status Report. Becker DP, Povlishock JT (eds.). North-Holland Publishing Co, NY. 463-473.

Young W, Flamm ES. (1982) Effect of high-dose corticosteroid therapy on blood flow, evoked potentials, and extracellular calcium in experimental spinal injury. J. Neurosurg. **57**: 667-673.

Discussion with Reviewers

K.P. Ryan: How was it known when the sections were freeze-dried? What time period elapsed?

Authors: The frozen grid/section is placed into the Gatan transfer device at -170°C and placed into the electron microscope and warmed to -120°C for 10 minutes. The specimen is warmed in 10°C increments every 10 minutes to -90°C. From -90°C, the specimen is warmed at 2°C each for 5 minutes until all regions of the grid are electron lucent to 40 μA, 125 keV beam at 30X magnification. The specimen is warmed to -80°C for 10 minutes and then cooled to -100°C for all analyses. After freeze drying, the grid is surveyed at low magnification, to locate a region for analysis, and the entire grid square is stabilized by irradiation with the electron beam for 10 minutes in the TEM mode. Stabilization is done with the X-ray detector retracted and the specimen flat to minimize the scattering of high energy electrons into the detector crystal. The area to be analyzed is then irradiated for 5 minutes in the STEM mode with slow scans at probing beam current. This stabilization procedure minimizes sample charging and movement and ensures that all mass loss is complete before analyses, and ensures that subsequent analyses of other experimental sections will have a predictable degree of reproducibility. After this stabilization process, areas can be repeatedly analyzed with no noticeable degradation or changes in the continuum count rate.

K.P. Ryan: The 400 second analysis times are not unusual for this type of work, I have used 300 seconds on frozen bulk material. Did you notice any change in the analysed areas of the sections, particularly thinning or, in other words, mass loss? Was the beam current reduced compared to normal imaging of resin sections? Were there any charge effects?

Authors: The question of "mass loss" is always troubling when one is attempting microanalytical analysis of diffusible ions in cryo-sections. The extent of hydration in the "dried" samples is unknown. The drying procedure was empirically derived to yield consistent samples. The specimen analysis temperature was also empirically derived. The added stability of low specimen temperature was balanced against the propensity of cold specimens to cryo-pump the microscope vacuum. Although a cold trap extends to within 5 mm of the sample, its temperature near the specimen is unknown. When analyzing the specimen at -120°C, we have observed sample etching when the level of liquid nitrogen in the cold trap was permitted to drop to 1 inch before refilling. While this is not standard practice, the effects of this error were not observed when analyzing at -100°C. The beam current was not reduced from the usual operating conditions for epoxy sections. Charging was not a problem when the carbon films were intact and the sample was well dried. Spectra that had degraded count rates in the continuum were discarded.

K.P. Ryan: What is the effect of the trauma in the animals that are not subsequently sacrificed?

Authors: Twenty gm/cm was the trauma that caused variable but permanent functional impairment (Tarlov score 3 or below) yet did not cause axotomy. Six gm/cm was a mild trauma and voluntary hind limb

movement was usually observed by 6 hour post trauma. In spite of these different physiological outcomes, the axons were remarkably similar. In both cases, the majority of axons were swollen while a number had condensed axoplasm. The electrolyte shifts that accompanied swelling and condensation were the same in both trauma doses. Chemically deranged axons could only be found after the more severe injury.

K. Zierold: Tables 1 and 2 show an increase in calcium in all measured compartments of the axons. Where does the calcium come from?
Authors: Our first assumption was that calcium sequesterization was a result of ischemia. In an effort to support or deny this hypothesis, we learned to grow organotypic spinal cords in culture (no blood supply), and subjected these cultures to various experimental conditions of trauma. Comparable changes in Ca were noticed in these cultures, putting the effects of ischemia into question. The nature of the anastomosing blood supply to the spinal cord also belies this notion. In short, we have not investigated the source of calcium further than our tissue culture model.

K. Zierold: How do you explain the increase of Fe in the traumatized axons?
Authors: We can only guess that the Fe increase is the result of ruptured blood vessels in the trauma animals. A variable number of trauma animals had surface as well as deep hemorrhages. No hemorrhages were noted in the sham operated animals.

K. Zierold: Are there differences in the elemental distribution after trauma in swollen and unswollen parts of the spinal cord?
Authors: We were surprised to find that major morphological changes, such as swelling, were not predictors of compositional changes, nor were these changes an indication of axon viability. That is, some of the non-functional axons, as judged by elemental analysis, appeared to be morphologically normal and some morphologically damaged axons (i.e., swollen) were compositionally within normal ranges.

K. Zierold: Have you measured the elemental distribution in the spinal cord cryofixed immediately after trauma?
Authors: One of the members in our group made atomic absorption (AA) measurements, early on, at different time periods following trauma (Banik et al., 1980, text reference). It was these measurements and morphological comparisons that alerted us to the marked increase in Ca by 6 hours post trauma. The AA measurements found no appreciable differences in the shams and 10

minutes post trauma. As a matter of fact, there was a decrease in Ca and an increase K immediately post trauma. This Ca drop was found to be in the extracellular compartment by Young [Young W. (1986) Ca paradox in neural injury: a hypothesis. Cent Nerv Syst Trauma 3: 235-251]. The blood flow remained unimpaired for the first few hours post trauma. We assume that the trauma causes the axons to be Ca and K permeable allowing free movement Other time points indicated that the calcium increase became the most noticeable 1 hour after trauma and peaked at 12 hours. We determined that the time period of 6 hours post trauma was important in terms of effecting a treatment.

K. Zierold: Do you have indications that anesthesia may have an effect on the elemental distribution?
Authors: The effect of Ketamine anesthesia on the elemental distribution in the spinal cord was not investigated in this laboratory. Meetings and eventual agreements on certain uniformities by investigators in spinal cord trauma research (animal models and anesthesia) has led to the present protocols. We have not deviated from these standards. A protocol to investigate the many facets of anesthesia might be very interesting but would probably not be fundable.